Kinetic Study of the Thermal Polymerization Reactions between Diazide and Internal Diyne

RONGPENG LIU, LIQIANG WAN, FARONG HUANG, LEI DU

Key Laboratory for Specially Functional Polymeric Materials and Related Technology of the Ministry of Education, School of Materials Science and Engineering, East China University of Science and Technology, Shanghai 200237, People's Republic of China

Received 19 June 2014; revised 16 November 2014; accepted 22 November 2014

DOI 10.1002/kin.20898

ABSTRACT: The reaction kinetics between diazide(4,4′-biphenyl dibenzyl azide) and internal diyne(bis[2-(phenyl)ethynyl]dimethylsilane) was studied in this study by means of differential scanning calorimetry (DSC) and nuclear magnetic resonance spectra (^{1}H NMR). DSC was carried out to analyze the reaction in bulk polymerization condition, whereas ^{1}H NMR for solution reaction polymerization. The apparent activation energy (e_α) calculated by Kissinger's method was 90.83 kJ/mol, which was confirmed by Friedman's method, and 87.67 kJ/mol by ^{1}H NMR, respectively. The polymerization between the diazide and internal diyne was the second-order reaction based on calculation from both of DSC and ^{1}H NMR. © 2014 Wiley Periodicals, Inc. Int J Chem Kinet 47: 124–132, 2015

INTRODUCTION

Cycloaddition reactions have been employed in polymer synthesis since the mid-1960s, using cycloaddition reactions for polymerization purposes allows rapid access to linear, hyperbranched, and dendritic architectures that feature interesting heterocyclic or strained multicyclic units within the polymer backbone. Cycloaddition reactions are very efficient and highly selective and allow even stereoselectivity. Polymers produced via cycloaddition chemistries have found use in several advanced applications such as liquid crystal displays, semiconductors, electrolyte membranes, and high-temperature performance polymers [1,2].

As a classical cycloaddition reaction, Micheal [3] discovered 1,3-dipolar cycloaddition in 1893, the reaction formed 1,2,3-triazole from phenyl azide and dimethyl acelenedicarboxylate. Since then, the 1,3-dipolar cycloaddition between alkyne and azide group has become an important method to synthesize 1,2,3-triazole compounds and their derivatives [4,5]. The mechanism of 1,3-dipolar cycloaddition between alkynes and azides was studied by Huisgen in 1960s, which formed 1,4-disubstituded and 1,5-disubstitued 1,2,3-triazoles [6]. In 1960s, Johson and colleagues synthesized several linear polytriazoles (PTAs) from monomers containing both azide and acetylene groups [7,8]. The obtained PTAs were thermally stable but

---

Correspondence to: Liqiang Wan; e-mail: wanliqiang@163.com

hardly processable polymers due to the rigid molecular chains.

Until 2001, the independent discovery of the copper(I)-catalyzed alkyne-azide 1,3-cycloaddition has been obtained by the Meldal [9] and Sharpless [10] groups; since then, hundreds of papers have appeared describing the use of this simple “click” methodology in diverse areas including drug discovery, bioconjugate chemistry, surface modification, materials preparation, and polyfunctionalized-building blocks. Its application in numerous areas has highlighted the value of its benign reaction conditions, functional tolerance, simple workup, and purification procedures. Hence, these long-neglected reactions were suddenly reestablished in organic synthesis and, in particular, have gained popularity in materials science nowadays [11–17].

Our laboratory has been engaged in developing novel low-temperature curing and heat-resistant resins by the 1,3-dipolar cycloaddition of azide with the alkyne group since 2002, which were polymerized at 80°C without Cu(I), a series of PTAs with good processability and thermal stability has been synthesized [18–22], and a series of novel polytriazoleimides (PTAIs) containing 1,2,3-triazole has been reported by thermal or chemical imidization methods, which exhibited high mechanical properties and chemical stabilities and were expected to be used as an advanced low-temperature molding materials [23,24]. In addition to PTAs and PTAIs, a novel PTA-based organogel has been formed by the effects of copper ions due to the advantages of the “click” reaction [25].

Although the reaction of internal alkyne and azide cannot be catalyzed by Cu(I), the reaction is also a useful method to prepare materials [26]. Kinetic studies and computational calculations have been reported about the internal alkyne and azide, the second-order reaction has been applied in this reaction [27–29]. In our previous study, the kinetics of 1,3-dipolar cycloaddition between diazide and different terminal diynes under thermal but copper-free conditions has been studied. To improve heat-resistant property, internal alkyne was used in PTA resins. So in this paper, to deeply understand the 1,3-dipolar cycloaddition of PTAs, the kinetics of the reaction between diazide and internal diyne was studied by differential scanning calorimetry (DSC) and nuclear magnetic resonance spectra (^{1}H NMR), respectively.

EXPERIMENTAL

Raw Materials

Magnesium powder, hexane (analytical grade (AR)), tetrahydrofuran (THF), dimethylfomamide (AR), bromoethane (AR), toluene (AR), hydrochloric acid (AR), dichloromethane (AR), and magnesium sulfate (anhydrous, AR) were purchased from Shanghai No.1 Reagent Company(Shanghai, China). Sodium azide (chemical pure (CP)) was purchased from Zhejiang Chengguan Chemical Reagent Factory(Zhejiang, China). 4,4′-Dichloromethylbiphenyl (technical pure (TP)) was purchased from Wuhan Chemical Reagent Factory(Wuhan, China). Dimethyldichlorosilane and dimethyl sulfoxide-d_6 (DMSO-d_6) were obtained from Aladdin Reagent (Shanghai, China). Phenylacetylent was obtained from Tokyo Chemical Industry (Shanghai, China). THF was refluxed over sodium with benzophenone and freshly distilled in nitrogen before use. 4,4′-Dichloromethylbiphenyl was recrystallized from methanol before use. Other chemicals were purchased and used as received without further purification.

Synthesis of 4,4′-Biphenyl Dibenzyl Azide (Diazide)

4,4′-Biphenyl dibenzyl azide was synthesized according to the method described in the literature [22]. 6.30 g 4,4′-dichloromethylbiphenyl, 6.50 g sodium azide, 20 mL dimethylformamide, and 20 mL toluene were added into a three-necked round-bottom flask (100 mL) with a mechanical stirrer and a reflux condenser. The reaction mixture was slowly heated to 75°C and kept at this temperature for 6 h. Then the reaction mixture was poured into a beaker with 200 mL deionized water. The organic layer was separated, and the aqueous layer was extracted with 20 mL toluene. The process was repeated three times. The organic benzene layers were combined and dried by anhydrous magnesium sulfate, and the toluene was then distilled. The spectroscopic data were consistent with the reported value. mp: 71–72°C; FT IR: 2109 cm^{-1} (–N$_3$); ^{1}H NMR: (CDCl$_3$, TMS): 7.39–7.42(d, 4H, Ar-H), 7.26–7.60 (d, 4H, Ar-H), 4.40 (s, 4H, Ar-CH$_2$N$_3$); ^{13}C NMR: (CDCl$_3$, TMS): 140.86, 135.07, 129.12, 128.88 (Ar), 54.85 (CH$_2$N$_3$); HRMS (EI, TOF) calcd for $C_{14}H_{12}N_6$ [M]$^+$ 264.1123; found 264.1125.

Synthesis of Bis [2-(phenyl)ethynyl]dimethylsilane (Internal Diyne)

Magnesium powder (2.88 g, 0.12 mol) and dry THF (30 mL) were added to a round-bottom flask through mechanical stirring and a condenser pipe. Bromoethane (13.08 g, 0.12 mol) dissolved in dry THF (30 mL) was added dropwise over 1 h to the magnesium suspension under room temperature. Then, the solution was refluxed for 1 h, after that phenylacetylene

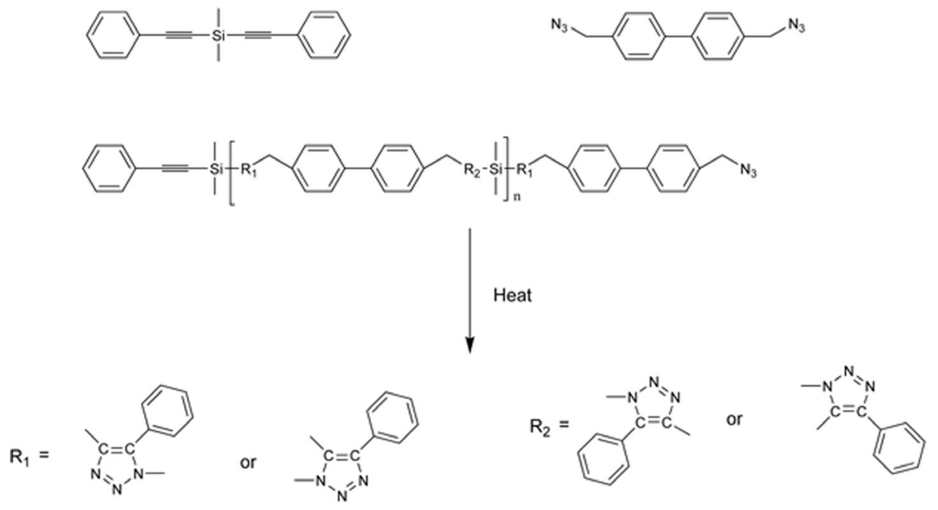

Figure 1 Synthesis route to 1, 3-dipolar cycloaddition between diazide and internal diyne.

(12.24 g, 0.12 mol) dissolved in dry THF (40 mL) was added slowly over 1 h under room temperature; the solution was refluxed for 1 h again. Dimethyldichlorosilane (6.19 g, 0.048 mol)dissolved in dry THF (30 mL) was added in three portions at ambient temperature, producing a gray-green precipitate; the suspension was refluxed for 1 h. After this, THF was distilled for about 100 mL. The flask was cooled in an ice bath, and the reaction was quenched with 2 wt% dilute hydrochloric acid (50 mL). The solution was extracted with 100 mL toluene; then the organic phase was washed with be neutral with water, separated, dried (anhydrous magnesium sulfate), and the solvent was removed in vacuum. The residue was recrystallized from hexane (3 × 20 mL) to afford the compound as off-white crystals (9.52 g, 0.025 mol, 75%). mp: 78–79°C; ^{1}H NMR: ($CDCl_3$, TMS): 7.53–7.56 (m, 4H, Ar-H), 7.31–7.39 (m, 6H, Ar-H), 0.53 (s, 6H, $Si(CH_3)_2$); ^{13}C NMR: ($CDCl_3$, TMS): 132.61, 129.37, 128.72, 123.15 (Ar), 106.43 (Ar–C≡C), 91.11 (C≡C–Si), 1.00 (Si–CH_3); HRMS (EI, TOF) calcd for $C_{18}H_{16}Si$ $[M]^+$ 260.1021, found 260.1020.

Analytical Methods

Proton nuclear magnetic resonance (^{1}H NMR) spectra were obtained from a Bruker Avance 500 (500 MHz) NMR spectrometer, and tetramethylsilane (TMS) was used as an internal standard. DSC measurement was carried out on a DSC TA Instruments DSC Q2000 spectrometer. The heating rate of 5, 10, 15, and 20 °C/min was chosen for the tests at a flow rate of nitrogen (50 cm^3/min).

Sample Preparation

For DSC kinetic studies, the samples were prepared by mixing diazide with internal diyne in a 1:1 molar ratio in 2 mL of dichloromethane at room temperature using a magnetic stirrer, then the solution was poured into a clean watch glass to evaporate the solvent. The samples were obtained after drying under vacuum at room temperature for 30 min, and prepared samples were stored in a freezer at –13°C in sealed vials for subsequent analysis.

For ^{1}H NMR kinetic studies, diazide and internal diyne were dissolved in a 25-mL round-bottom flask with 4 mL DMSO-d_6 at temperatures ranging from 80 to 110°C through magnetic stirring. And then the step-growth coupling reactions were monitored. At regular time intervals, 200 μL of reaction mixture was withdrawn and dissolved in 0.3 mL of DMSO-d_6. The time-conversion studies were then calculated by integration of ^{1}H NMR spectra.

RESULTS AND DISCUSSION

Kinetic Study by DSC

The sample of diazide and internal diyne as shown in Fig. 1 were examined in a DSC cell from 20 to 300°C at a heating rate of 5, 10, 15, and 20°C/min under nitrogen atmosphere. Fig. 2 shows a series of dynamic scanning thermograms for diazide and internal diyne.

As shown in Fig. 2, endothermic peaks appear around 50°C, which are ascribed to the melting of the solid reactants. Then the exothermic peaks are

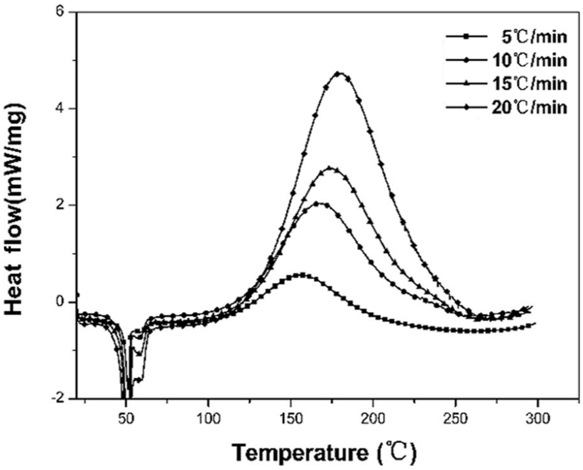

Figure 2 DSC thermograms for diazide and internal diyne at different heating hates.

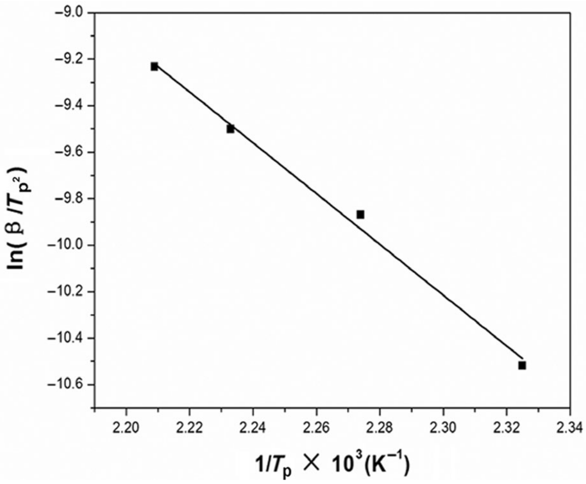

Figure 3 Kissinger's analysis for diazide and internal diyne.

Table I DSC Results of the Diazide and Internal Diyne Reaction

Heating rate (β) (°C/min)	Peak Temperatures, Tp(°C)	ΔH (J/g)
5	157.05	883.4
10	166.65	901.3
15	174.75	836.3
20	179.45	934.0

observed in the temperature ranging from 100 to 300°C, which is due to the 1,3-dipolar cycloaddition. The values of reaction heat (ΔH) obtained from the scans at different heating rates are slightly different and summarized in Table I.

Generally, with the increment of heating rates, peak temperatures shift to higher temperatures. Kissinger's equation is used to calculate the activation energy as the equation is described below [30]:

$$\ln\left(\frac{\beta}{T_P^2}\right) = \ln\left(\frac{AR}{E_\alpha}\right) - \frac{E_\alpha}{RT_P} \tag{1}$$

In Eq. (1), where R is the universal gas constant, A is the preexponential factor, β is the heating rate, T_{P} is the peak temperatures, and $\ln(\mathrm{AR}/E_\alpha)$ is a constant. So a plot of $\ln(\beta/T_{\mathrm{P}}{}^2)$ against $1/T_{\mathrm{P}}$ yields values for E_α from the slope of the liner fit with a coefficient of determination $R^2 > 0.99$, as shown in Fig. 3. The E_α of diazide and internal diyne reaction are calculated as 90.83 kJ/mol.

Besides using Kissinger's equation, the differential isoconversional method was also employed to confirm the accuracy of the E_α calculated by Kissinger's method. The most common differential isoconversional method is that of Friedman [31], based on Eq. (2):

$$\ln\left(\frac{\mathrm{d}\alpha}{\mathrm{d}t}\right)_\alpha = \ln[f(\alpha)A_\alpha] - \frac{E_\alpha}{RT_\alpha} \tag{2}$$

For linear nonisothermal programs, Eq. (2) is frequently used in the following form:

$$\ln\left(\beta\frac{\mathrm{d}\alpha}{\mathrm{d}T}\right)_\alpha = \ln[f(\alpha)A_\alpha] - \frac{E_\alpha}{RT_\alpha} \tag{3}$$

From Eq. (3), the relationship between E_α and the extent of conversion α can be achieved. The results are illustrated in Fig. 4 for diazide and internal diyne.

Fig. 4 indicates that the E_α is stable with the increment of extent of conversion (α) when α is lower than 80%. Then E_α increases gradually, which is due to the decomposition of the azide group. The average data of E_α is 89.61 kJ/mol when α is lower than 80%, which is very close to the values calculated by Kissinger's method.

The DSC method not only provides the value of E_α but also indicates further details of reaction kinetics such as reaction order through model fitting.

$$\beta\frac{d\alpha}{dT} = A\exp\left(-\frac{E_a}{RT}\right)(1-\alpha)^n \tag{4}$$

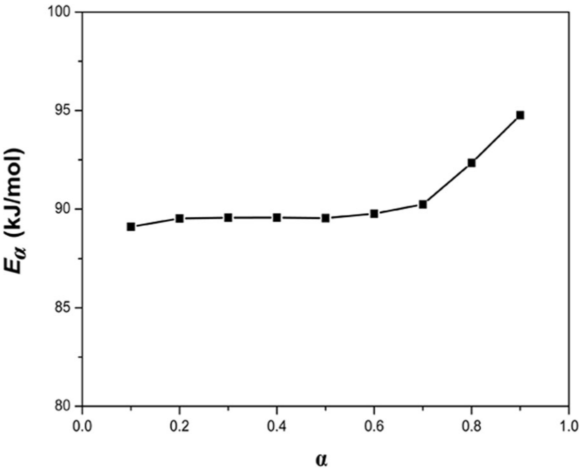

Figure 4 Relationship between E_α and α for diazide and internal diyne.

The reaction model described as Eq. (4) [from Eq. (3)] can be used to fit the experimental data, which can be used to obtain the reaction order, *n*.

To simplify the calculation, the constant value of E_α from Kissinger's analysis is considered in Eq. (4). A plot of $\ln[\beta(\mathrm{d}\alpha/\mathrm{d}T)] + \ln(E_\alpha/RT)$ against $\ln(1–\alpha)$ yields values for the preexponential factor *A* and reaction orders *n* from the intercept and slope of the liner fit, respectively. Fig. 5 demonstrates the *n*th-order model-fitting curves of diazide and internal diyne reaction at 5, 10, 15, and 20°C/min, respectively. In these cases, the model curves are consistent with the experimental data; whereas at the end of the reaction, the model curves deviate from the experimental data, which are ascribed to the change in E_α as shown in Fig. 4.

The kinetic parameters for bulk polymerization of diazide and internal diyne are calculated and listed in Table II. As discussed above, the reaction of diazide and internal diyne meets the *n*th-order model, which shows a near second-order reaction characteristic. In our previous study, the kinetics of diazide and two terminal diynes was studied [32]; the E_α of diazide and internal diyne is a little higher than those of diazide and terminal diynes because of maybe larger

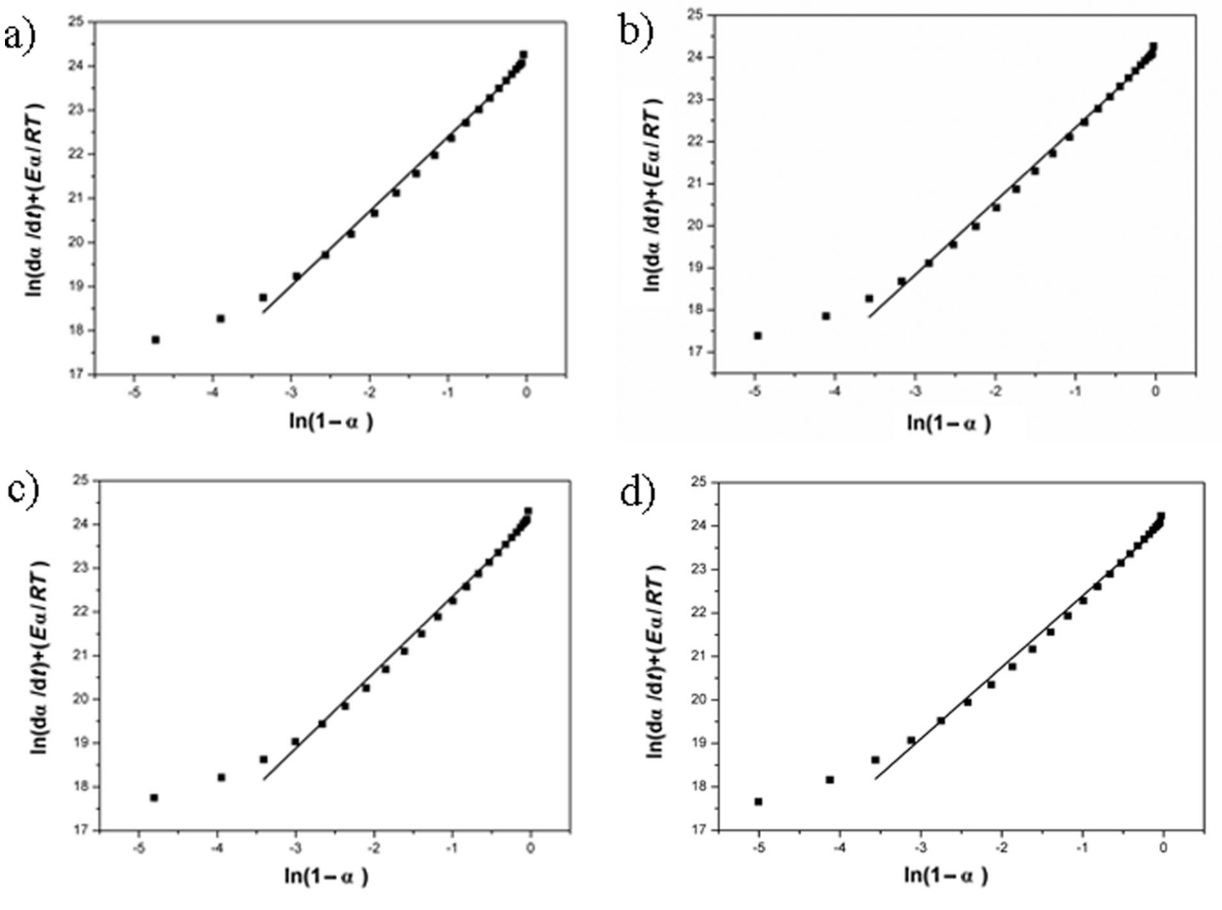

Figure 5 The *n*th model fits of diazide and internal diyne at (a) 5°C/min, (b) 10°C/min, (c) 15°C/min, and d) 20°C/min.

Table II Summary of the Kinetic Parameters of Diazide and Internal Diyne Reaction

Sample	A ($\times 10$)[a]	n[a]	E[b](kJ/mol)	E[c](kJ/mol)
5°C/min	2.90	1.69	90.83	89.61
10°C/min	2.88	1.75		
15°C/min	2.90	1.74		
20°C/min	2.76	1.65		

[a] Values from the fitting parameters of original experimental data.
[b] Calculated from Kissinger's method.
[c] Calculated from Friedman's method.

steric hindrance of internal diyne or a different reaction mechanism. For diazide and terminal diynes, the reactions are both first-order reactions, which indicates that the reaction between diazide and internal diyne, diazide, and terminal diyne possesses different mechanisms.

Table III Observed Rate Orders in the Variable Component Derived from Kinetic Measurements[a]

Component	[Internal Diyne] [M]	[Diazide] [M]	Rate Order
Internal diyne	0.5–1.5	0.5	0.82
diazide	0.5	0.5–1.5	0.75

[a] Reactions were performed at 100 ±1°C in DMSO.

Kinetic Study by ^{1}H NMR

To study the reaction kinetics via solution polymerization, ^{1}H NMR is used to determine the changes in monomers during the 1,3-dipolar cycloaddition.

As shown in Fig. 6, through changing a single reactant, the contribution of internal diyne and diazide for the reaction is calculated, respectively. By means of plotting the initial reaction rate against reactant conversion, the reaction orders of internal diyne and diazide shown in Table III are both near first orders, which

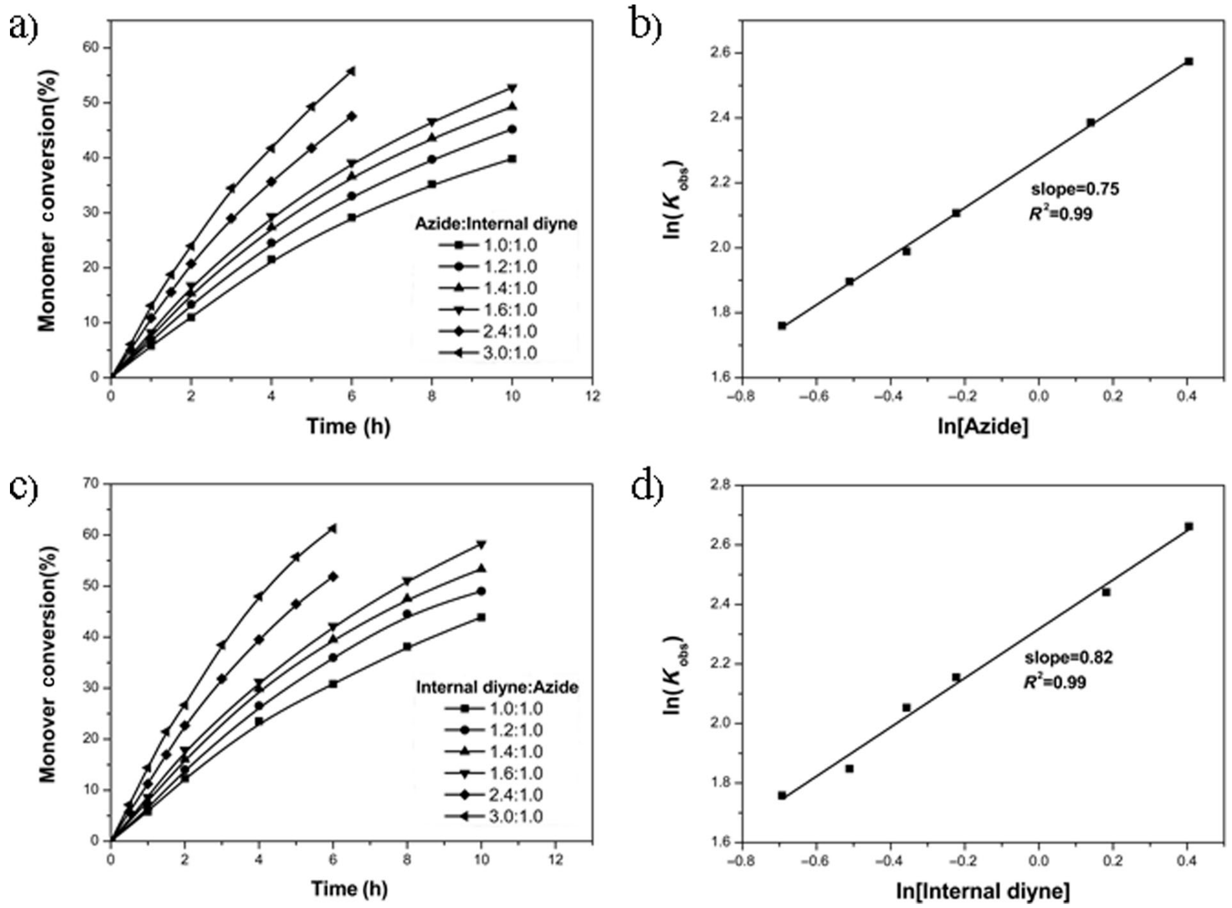

Figure 6 Kinetic measurements: (a) the relationship between [azide] and monomer conversion, (b) rate-order plots showing the first-order dependence on [azide], (c) the relationship between [internal diyne] and monomer conversion, and (d) rate-order plots showing the first-order dependence on [internal diyne].

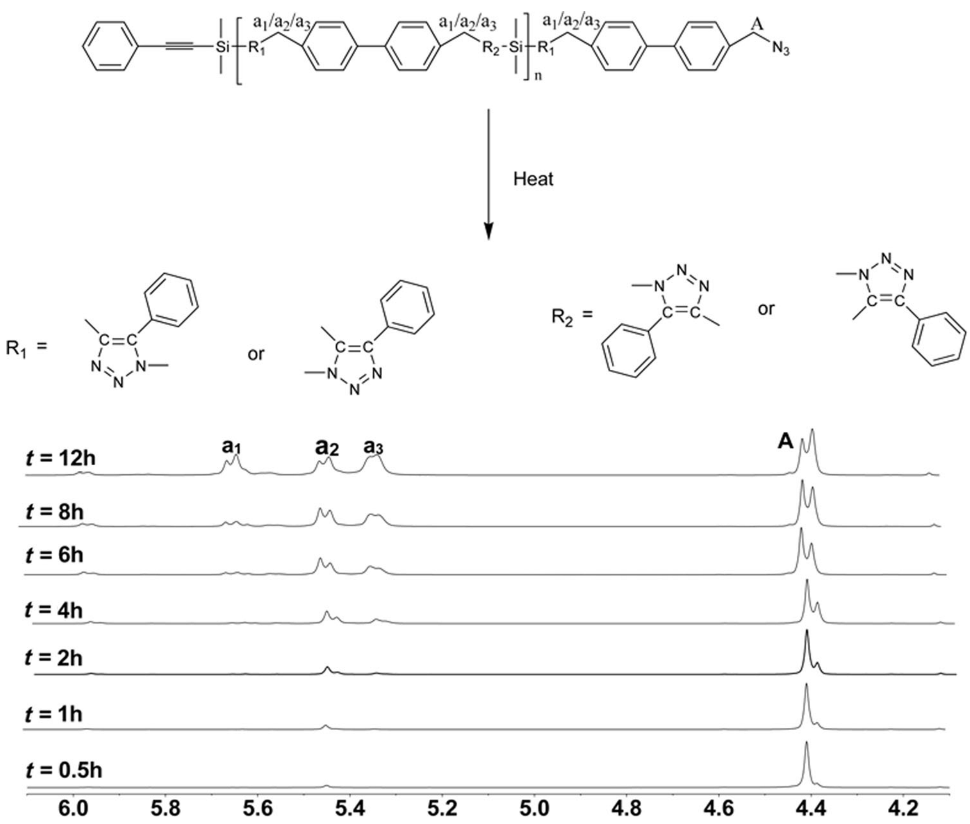

Figure 7 Evolution of ^{1}H NMR spectra (DMSO-d_6, [internal diyne]/[azide] = 1.6:1.0, and $T = 100$°C) during the synthesis of diazide and internal diyne.

implies that the 1,3-dipolar cycloaddition of internal diyne and diazide is a second-order reaction.

In detail, the polymerization kinetics of a 1:1 molar ratio of diazide and internal diyne in DMSO-d_6 was monitored by ^{1}H NMR spectroscopy at 80, 90, 100, and 110°C, respectively. The reaction evolution of the 1,3-dipolar cycloaddition between diazide and internal diyne is shown in Fig. 7. For diazide and internal diyne, the reaction was confirmed by the signal shift from methylene groups adjacent to azide (at 4.40 ppm) toward the methylene protons adjacent to the formed triazole rings (at 5.34, 5.45, 5.65 ppm).

Conversion ratios of the monomers are calculated by integration of the ^{1}H NMR spectra. Following the evolutions azide and triazole signals, the reaction degree can be described as follows:

$$a = \frac{Ia_1 + Ia_2 + Ia_3}{I_A + Ia_1 + Ia_2 + Ia_3}$$

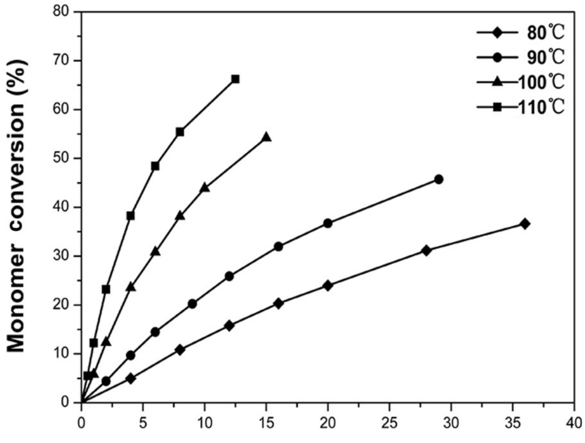

Figure 8 ^{1}H NMR monitoring (DMSO-d_6, 0.5 mol/L of monomers at $T = 80$, 90, 100, and 110°C) for the reaction of diazide and internal diyne.

where α is the conversion at t time, and Ia_1, Ia_2, and Ia_3 are the integration of signal related to methylene protons adjacent to the formed triazole rings, whereas I_A is the integration of signal corresponding to the methylene groups adjacent to azide. The conversion rates of a triazole unit at 80, 90, 100, and 110°C for diazide and internal diyne are presented in Fig. 8.

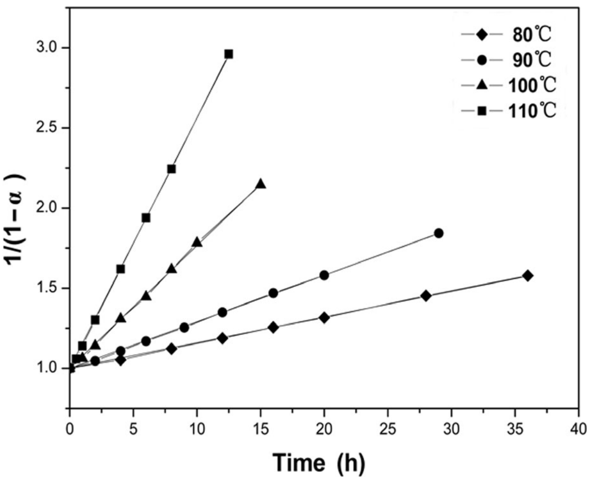

Figure 9 Second-order linearization plots for the synthesis of diazide and internal diyne (DMSO-d_6, 0.5 mol/L of monomers at $T = 80$, 90, 100, and 110°C), where α is the monomer conversion.

Moreover, as shown in Figs. 9 and 10, the second-order linearization of the time-conversion plots provides the determination of the overall polymerization rate constant k for each temperature. Arrhenius' plot of these data with a coefficient of determination $R^2 > 0.99$ allows calculation of the E_α of the 1,3-dipolar cycloadditions, which is 87.67 kJ/mol for diazide and internal diyne. All the kinetic parameters are summarized in Table IV.

Kinetic parameters calculated with ^{1}H NMR analysis are consistent with that achieved by means of the DSC method. However, the reaction order and E_α are quite different from the reaction for diazide and terminal diynes. Both of the reactions between diazide and terminal diynes are the first-order reactions, whereas diazide and internal diyne is a second-order reaction. The reason of the different reaction orders of internal alkyne/azide and terminal alkyne/azide is the different rate-determining steps for the concerted 1,3-dipolar cycloaddition. Achieving a transition state geometry requires significant distortion of the dipole and the dipolarophile distortion. For an internal alkyne/azide reaction, due to the lager steric hindrance of internal alkyne, its distortion is much difficult than that of terminal alkyne; the rate-determining step changes and causes different reaction mechanism. Furthermore, for diazide and terminal diynes, owing to faster mobility of monomers and more effective molecular collisions, the functional groups have much higher reactivity in the solution. Then the obtained E_α from ^{1}H NMR are much lower than those form DSC, is about 10 kJ/mol. However, in the reaction of diazide and internal diyne, the E_α from ^{1}H NMR is a little lower (about 2 kJ/mol) than that from DSC; the result implies that the polymerization carried out in the solution reaction is not easier than that of terminal diynes.

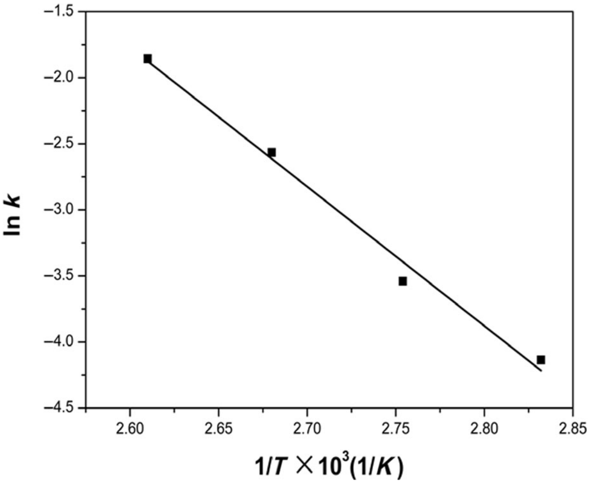

Figure 10 ln k-T^{-1} plots for the reaction of diazide and internal diyne.

Table IV Summary of the Kinetic Parameters of Internal Diyne and Diazide under Different Temperatures

Temperature (°C)	k ($M^{-1}\cdot h^{-1}$)	R^2
80	0.01598	0.99
90	0.02901	0.99
100	0.07688	0.99
110	0.1562	0.99

CONCLUSIONS

The reaction kinetic of bulk and solution polymerization without copper catalysts between diazide and internal diyne was studied by DSC and ^{1}H NMR, respectively. The results show that

(a) the E_α obtained from ^{1}H NMR spectra was close to that by the DSC method, about 10 kJ/mol is higher than the reactions for diazide and terminal diynes;

(b) The reaction for diazide and internal diyne is a second-order reaction, which is totally different from the first-order reaction for diazide and terminal diynes, described in the literature before.

The authors gratefully acknowledge the financial support of Shanghai Leading Academic Discipline Project (B502) and Fundamental Research Funds for the Central University.

BIBLIOGRAPHY

1. Brigitte Voit, New J Chem 2007, 31, 1139–1151.
2. Goodall Glenn, W.; Wayne Hayes, Chem Soc Rev 2006, 35, 280–312.
3. Micheal, A. J Prakt Chem 1893, 48, 94–95.
4. Benson, F. R.; Savel, W. L. Chem Rev 1950, 46, 1–68.
5. L'abbe, G. Chem Rev 1969, 69, 345–363.
6. Huisgen, R. Angew Chem, Int Ed 1963, 2, 565–632.
7. Johson, K. E.; Lovinger, J. A.; Parker, C. O.; Baldwin, M. G. J Polym Sci, Part B: Polym Lett 1966, 4, 977–979.
8. Baldwin, M. G.; Johson, K. E.; Lovinger, J. A. J Polym Sci, Part B: Polym Lett 1967, 5, 803–805.
9. Tornøe, C. W.; Christensen, C.; Meldal, M. J Org Chem 2002, 67, 3057–3062.
10. Rostovtsev, V. V.; Green, L. G.; Fokin, V. V., Sharpless, K. B. Angew Chem, Int Ed 2002, 41, 2596–2599.
11. Binder, W. H.; Sachsenhofer, R. Macromol Rapid Commun 2008, 29, 952–981.
12. Iha, R. K.; Wooley, K. L.; Nyström, A. M., Burke, D. J.; Kade, M. J.; Hawker, C. J. Chem Rev 2009, 109, 5620–5686.
13. Morten, M.; Tornøe, C. W. Chem Rev 2008, 108, 2952–3015.
14. Carlmark, A.; Hawker, C.; Hult, A.; Malkoch, M. Chem Soc Rev 2009, 38, 352–362.
15. Droumaguet, B. L.; Velonia, K. Macromol Rapid Commun 2008, 29, 1073–1089.
16. Jean-Francois, L. Angew Chem, Int Ed 2007, 46, 1018–1025.
17. Schunack, M.; Gragert, M.; Döhler, D.; Michael, P.; Binder, W. H. Macromol Chem Phys 2012, 213, 205–214.
18. Hu, Y. H.; Luo, Y. H.; Wan, L. Q.; Qi, H. M.; Huang, F. R.; Du, L. Acta Polym Sin 2005, 4, 560–565.
19. Luo, Y. H.; Hu, Y. H.; Wan, L. Q.; Xue, L.; Zhou, W.; Huang, F. R.; Shen, X. N.; Qi, H. M.; Du, L.; Chen, X. B. Chem J Chin Univ 2006, 27, 170–173.
20. Xue, L.; Wan, L. Q.; Hu, Y. H.; Shen, X. N.; Huang, F. R. Thermochim Acta 2006, 448, 147–153.
21. Tian, J. J.; Wan, L. Q.; Huang, J. Z.; Hu, Y. H.; Huang, F. R.; Du, L. Polym Adv Technol 2007, 18, 556–561.
22. Wan, L. Q.; Luo, Y. H.; Xue, L.; Tian, J. J.; Hu, Y. H.; Qi, H. M.; Shen, X. N.; Huang, F. R.; Du, L.; Chen, X. B. J Appl Polym Sci 2007, 104, 1038–1042.
23. E, Y. P.; Wan, L. Q.; Zhou, X. A.; Huang, F. R.; Du, L. Polym Adv Technol 2012, 23, 1092–1100.
24. E, Y. P.; Wan, L. Q.; Li, Y. J.; Huang, F. R.; Du, L. J Korean Chem Soc 2012, 33, 2193–2199.
25. Li, Y. J.; Wan, L. Q.; Zhou, H.; Huang, F. R.; Du, L. Polym Chem 2013, 4, 3444–3447.
26. Scheel. A. J.; Komber, H.; Voit, B. I. Macromol Rapid Commun 2004, 25, 1175–1180.
27. Ess, D. H.; Jones, G. O.; Houk, K. N. Org Lett 2008, 10, 1633–1636.
28. Liang, Y.; Mackey, J. L.; Lopez, S. A.; Liu, F.; Houk, K. N. J Am Chem soc 2012, 134, 17904–17907.
29. Gordon, C. G.; Mackey, J. L.; Jewett, J. C.; Sletten, E. M.; Houk, K. N.; Bertozzi, C. R. J Am Chem soc 2012, 134, 9199–9208.
30. Akahira, T.; Sunose, T. Res Rep, Chiba Inst Technol 1971, 16, 22–31.
31. Friedman, H. L. J Polym Sci, Part C 1964, 6, 183–195.
32. Liu, R. P.; Wan, L. Q.; Huang, F. R.; Du, L. J Wuhan Univ Technol (accepted).